Materials Science and Engineering A 527 (2010) 5723–5727

Contents lists available at ScienceDirect

Materials Science and Engineering A

journal homepage: www.elsevier.com/locate/msea

Enhanced mechanical properties of friction stir welded dissimilar Al–Cu joint by intermetallic compounds

P. Xue, B.L. Xiao, D.R. Ni, Z.Y. Ma*

Shenyang National Laboratory for Materials Science, Institute of Metal Research, Chinese Academy of Sciences, 72 Wenhua Road, Shenyang 110016, China

ARTICLE INFO

Article history:
Received 12 March 2010
Received in revised form 11 May 2010
Accepted 19 May 2010

Keywords:
Friction stir welding
Aluminum
Copper
Dissimilar joint
Intermetallic compounds

ABSTRACT

Aluminum and copper plates were successfully friction stir welded by offsetting the tool to the aluminum side, producing excellent metallurgical bonding on the Al–Cu interface with the formation of a thin, continuous and uniform Al–Cu intermetallic compound (IMC) layer. Furthermore, many IMC particles were generated in the nugget zone, forming a composite structure. Tensile tests indicated that the FSW joint failed in the heat-affected zone of the aluminum side with the Al–Cu interface bonding strength being higher than 210 MPa.

1. Introduction

The joining of dissimilar materials is becoming increasingly important in industrial applications due to their numerous advantages. These include not only technical advantages, such as desired product properties, but also benefits in terms of production economics [1]. Therefore, the sound joining technique of dissimilar materials is indispensable. However, dissimilar metals are difficult to join with conventional fusion welding due to their different chemical and physical characteristics, thus solid state joining methods have received much attention [2–8].

In the past decade, much attention has been directed towards friction stir welding (FSW) [9]. FSW is a revolutionary joining process, patented by The Welding Institute (TWI) of the UK [10] that has been shown to be an effective way of joining materials with poor fusion weldability, such as high-strength aluminum alloys and magnesium alloys [9]. Recently, attempts have been made to join dissimilar alloys through FSW, such as aluminum to steel, aluminum to magnesium, and aluminum to copper [11–17]. As a new solid state joining technology, FSW has a high possibility of making high-quality dissimilar welds compared to fusion welding. However, previous studies indicated that few sound dissimilar FSW joints were obtained. Usually, the dissimilar FSW joints failed at the nugget or along the interface between the two materials during the mechanical tests [11–15]. Therefore, it is worthwhile to study the detailed microstructures of the nugget and the bonding interface of dissimilar FSW joints.

It was well documented that for dissimilar Al–Cu joints fabricated by various joining methods, such as friction welding, explosive welding, and roll welding [4–8], an intermetallic compound (IMC) layer usually formed on the Al–Cu interface. A thick IMC layer would increase the brittleness of the interface, leading to easier crack initiation and propagation [8]. For FSW joints of dissimilar metals, it was reported that IMCs were easily formed in the nugget zone due to severe plastic deformation and thermal exposure [13–17]. Similar to other joining methods, when IMCs were excessively generated, the dissimilar FSW joints usually exhibited poor mechanical properties due to the inherent brittle nature of the IMCs [13–16]. Therefore, preventing the formation of excessive IMCs is extremely important in FSW of dissimilar materials. However, it is well known that IMCs have been used as reinforcing particles in metal matrix composites (MMCs). Moreover, Kao and coworkers produced several in situ aluminum matrix composites, reinforced by Al_2Cu [18], Al_3Ti [19], and Al–Fe IMCs [20], respectively, via friction stir processing (FSP), which is a microstructure modification processing based on the basic principles of FSW [9]. During FSW of dissimilar metals, stirring one type of metal particles into another metal matrix forming IMC particles is inevitable. In this case, it is very likely that these IMC particles exert a strengthening effect on the nugget zone. Therefore, the control of the IMC layer between dissimilar metals and the size and distribution of the IMC particles in the nugget zone becomes a key factor for FSW of dissimilar metals. However, detailed microstructural investigation

* Corresponding author. Tel.: +86 24 83978908; fax: +86 24 83978908.
E-mail address: zyma@imr.ac.cn (Z.Y. Ma).

0921-5093/$ – see front matter © 2010 Elsevier B.V. All rights reserved.
doi:10.1016/j.msea.2010.05.061

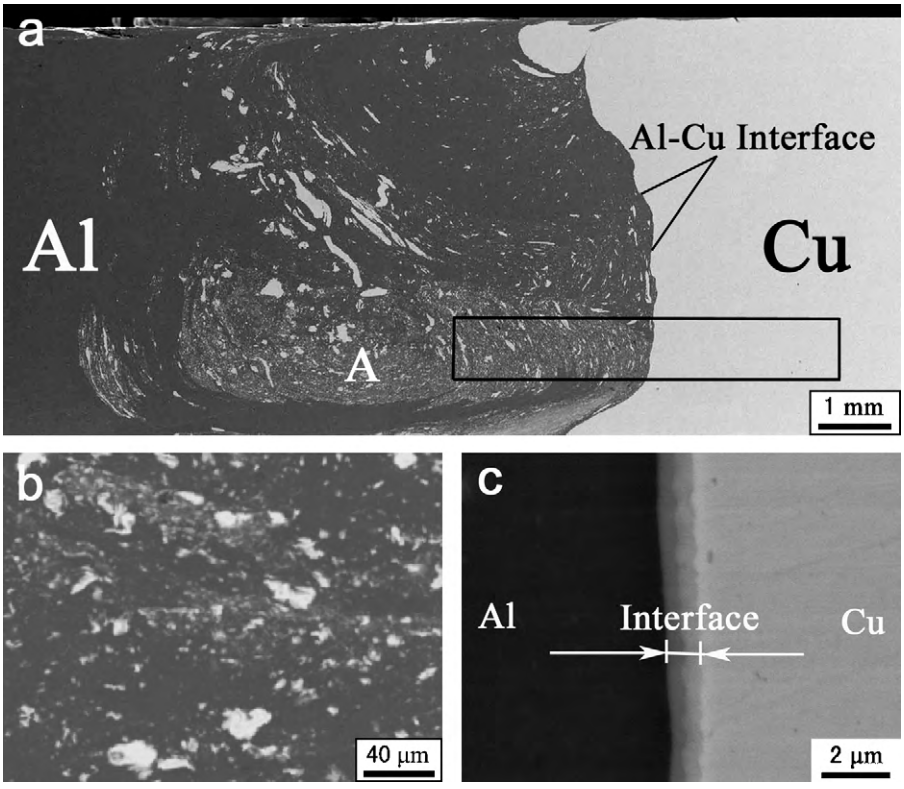

Fig. 1. SEM backscattered electron images (BEI) of the FSW Al–Cu joint: (a) cross-sectional macrograph of the joint, (b) magnified view of region A as marked in (a), and (c) microstructure of the Al–Cu interface. The rectangular region shows the gauge area of the mini tensile specimen.

on dissimilar metal interface and IMC particles in the nugget zone of FSW dissimilar metal joints is still lacking.

In this paper, sound FSW Al–Cu joints were successfully achieved by offsetting the tool to the aluminum side and controlling the FSW parameters, and the microstructures of the nugget zone and the bonding interface were analyzed in detail. The purpose of this study is to elucidate the correlation between the IMCs, formed during FSW, and bonding strength in dissimilar FSW joints.

2. Experimental procedures

1060 aluminum and commercial pure copper (99.9% purity, annealed) plates 5 mm in thickness, 300 mm in length, and 70 mm in width were butt-welded using a gantry FSW machine (China FSW Center). Unlike conventional friction stir butt welding, the tool pin was mostly offset into the aluminum side in this study in order to obtain defect-free joints and reduce the formation of the IMCs. Therefore, the pin stirred mainly in the aluminum during FSW process. FSW was conducted at a tool traverse speed of 100 mm min^{-1} and a rotation rate of 600 rpm.

Microstructural characterization and analyses were carried out by electron probe microscopic analyzer (EPMA), X-ray diffraction (XRD), scanning electron microscopy (SEM), and transmission electron microscopy (TEM), complemented by energy-dispersive spectroscopy (EDS). In order to identify the phase component of the interface layer by XRD, a sample that contains Cu bulk and a thin layer of the nugget zone was machined parallel to the Al–Cu interface from the upper part of the joint. Then the sample was dissolved in a hydrofluoric acid solution until part of the interface layer was exposed (the color of the interface layer was obviously different from the nugget zone). XRD examinations were performed on the sample surface before and after dissolving.

Large transverse tensile specimens with a gauge length of 40 mm and a width of 10 mm were machined perpendicular to the FSW direction. Meanwhile, for the sake of obtaining the bonding strength of the Al–Cu interface, mini tensile specimens of 5 mm gauge length, 1.5 mm gauge width and 0.8 mm gauge thickness were also machined perpendicular to the FSW direction with the Al–Cu interface in the gage center, as shown in Fig. 1a by the rectangle. Tensile tests were carried out at an initial strain rate of 1×10^{-3} s^{-1}. The Vickers microhardness tests were performed on the cross-section perpendicular to the welding direction using 200 g load for 10 s. Three-point bending tests were performed over a 40 mm span using a universal testing machine with a crosshead speed of 0.5 mm min^{-1}.

3. Results and discussion

Fig. 1 shows the SEM macroscopic appearance and the microstructures of the Al–Cu joint. As shown in Fig. 1a, the nugget zone consists of a mixture of the aluminum matrix and Cu particles (this will be discussed later). The distribution of Cu particles with irregular shapes and various sizes was inhomogeneous in the nugget zone and a particles-rich zone (PRZ) was formed near the bottom. Fig. 1b shows a magnified view of the PRZ. Many fine particles with various sizes are dispersed in the Al matrix, and some large particles can be also found. Thus, the nugget zone can be considered the aluminum matrix composite. The particles in the aluminum matrix of the nugget zone are attributed to the tool pin's stir action that scraped Cu pieces from the bulk copper, breaking up and dispersing them during FSW process.

Magnified view of the Al–Cu interface is shown in Fig. 1c. A continuous and uniform interface layer with a thickness of ~1 μm, consisting of two discernible sub-layers, is distinctly visible between Al and Cu bulk. Fig. 2a shows the XRD results of the Al–Cu interface. Only Al and Cu were clearly detected before dissolving in the hydrofluoric acid solution. However, the characteristic diffraction peaks of Al_2Cu and Al_4Cu_9 were clearly detected

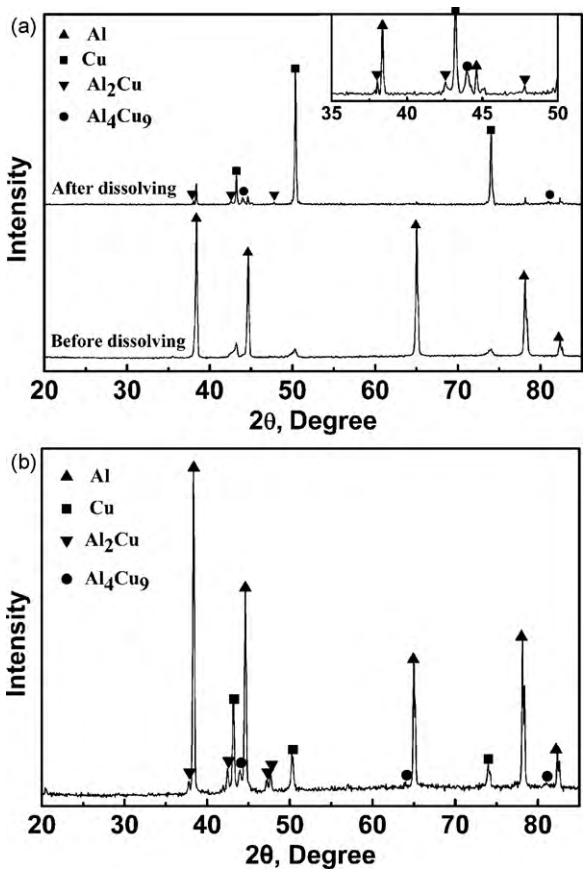

Fig. 2. X-ray diffraction patterns of (a) the Al–Cu interface and (b) the PRZ.

in the sample after dissolving, indicating that the Al–Cu interface layer was composed of Al_2Cu and Al_4Cu_9. According to the Al–Cu binary equilibrium phase diagram [21], several Al–Cu IMCs, including Al_2Cu (θ), AlCu (η_2), Al_3Cu_4 (ζ_2), Al_4Cu_9 (γ_1), may be developed during the Al/Cu reaction. Some studies indicated that during the Al/Cu reaction Al-rich phase Al_2Cu and Cu-rich phase Al_4Cu_9 were the first two IMCs formed adjacent to Al side and Cu side, respectively [8,22,23]. Therefore, the sub-layer near the copper side, as shown in Fig. 1c, should be Al_4Cu_9 and the other near the aluminum side should be Al_2Cu. In-depth TEM examination is in progress to elucidate the fine microstructure of the Al–Cu interface.

The element distribution maps of the PRZ shown in Fig. 1b were obtained by EPMA. According to the element distribution maps of Al and Cu in Fig. 3a and b, the larger bright particles shown in Fig. 1b were mainly composed of Cu element. However, the smaller particles had been transformed into the Al–Cu IMCs from the element distribution maps, and the IMC layers could be also observed around the larger particles. Moreover, XRD analysis on this zone (shown in Fig. 2b) revealed the existence of distinct characteristic diffraction peaks of Al_2Cu and Al_4Cu_9. Therefore, it is clear that Al_2Cu and Al_4Cu_9 were generated around the larger Cu particles, and for the smaller Cu particles most of copper were transformed into these two IMCs.

TEM microstructures of the IMCs in the PRZ are shown in Fig. 4. As shown in Fig. 4a, many interconnected particles were found in the PRZ, corresponding to the light gray particles revealed by SEM, Fig. 1b. Furthermore, there were also dispersed particles in the PRZ as shown in Fig. 4b. Most particles in the PRZ were identified as either Al_2Cu or Al_4Cu_9 by selected area diffraction (SAD) and EDS, which is in agreement with the XRD results (Fig. 2b). Besides, few particles in the PRZ were determined to be AlCu based on the EDS results and SAD patterns shown in Fig. 4c and d. Therefore, the IMC particles of the composite in the FSW Al–Cu joint were Al_2Cu, Al_4Cu_9 and AlCu, and this is quite different from the Al–Al_2Cu composite prepared from Al–Cu sinter via FSP in which only Al_2Cu particles were found [18].

The representative transverse cross-section hardness profiles measured along the top, the middle, and the bottom of the welded plate are showed in Fig. 5. The hardness values in the nugget zone exhibit an inhomogeneous distribution. The higher hardness values in the nugget zone than those in the Al base are attributed to the existence of variously sized Cu particles and the IMCs (Figs. 1, 3 and 4). The extremely high hardness value (126 HV) in the bottom of the nugget zone is even higher than that in the Cu base (~80 HV), so the particles in this area should be Al–Cu IMCs other than Cu particles. Ouyang et al. [16] indicated that the hardness of Al–Cu IMCs was much higher than that of Cu. Moreover, the hardness profiles at the Al side and Cu side were obviously different outside the nugget zone. The minimum hardness appears around 3–4 mm from the weld centre at the Al side, which corresponds to the heat-affected zone (HAZ). However, no obvious HAZ was observed at the Cu side, which should be attributed to the work hardening effect of the tool action during FSW, considering that the Cu plate was under softened condition due to annealing prior to FSW. A similar phenomenon was also observed in FSW Al alloy–stainless steel joint [11].

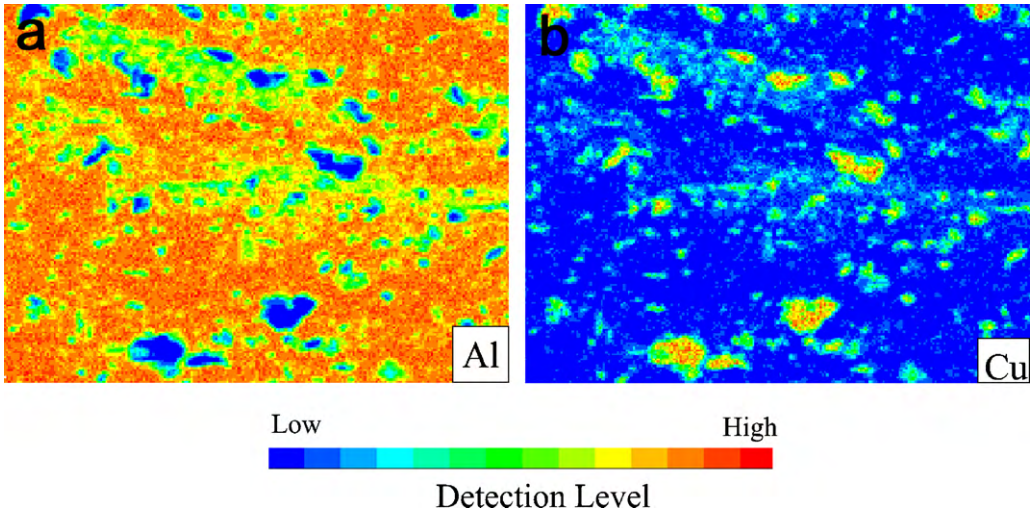

Fig. 3. Element distribution maps of the PRZ shown in Fig. 1(b): (a) Al element and (b) Cu element.

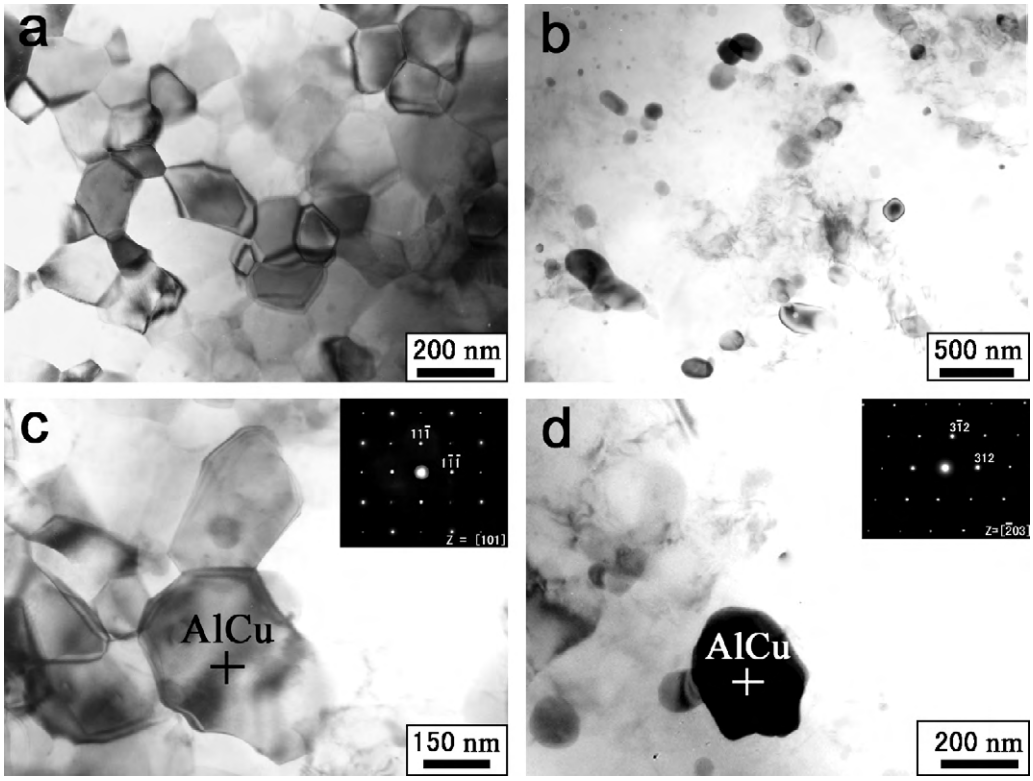

Fig. 4. TEM micrographs showing the morphologies of (a) the interconnected IMC particles, and (b) the dispersed IMC particles, (c) and (d) AlCu particles.

Table 1 illustrates the tensile properties of the FSW Al–Cu joints, as well as the Al base material (BM). The large tensile specimen of the Al–Cu joint fractured at the HAZ of the Al side with a high elongation (13%). The ultimate tensile strength (UTS) and yield strength (YS) are ~90% and ~80% of the Al BM, respectively, and slightly lower than those of the Al BM due to annealing softening during FSW. The mini-specimen fractured at the PRZ, and the UTS could get to 210 MPa which was much higher than the Al BM. The UTS of the Al-Fe composite produced by Lee et al. were 207 and 217 MPa after two passes and four passes FSP, respectively [20]. Clearly, similar strengthening effect in the PRZ was obtained by the Al–Cu IMCs for the present FSW Al–Cu joint. According to the discussion of Hsu et al. [19], the major contributions to the high strength of the composite structure are the fine grain size of the Al matrix and the Orowan strengthening due to the dispersion of the fine IMC particles. From the hardness profiles in Fig. 5, it is obvious that the hardness values in the PRZ are much higher than those of the area with no/few strengthening particles (similar to Al base of ~40 HV) in the upper nugget zone. Therefore, the Orowan strengthening by the dispersed IMC particles plays the key role in the strengthening mechanism of the present composite structure.

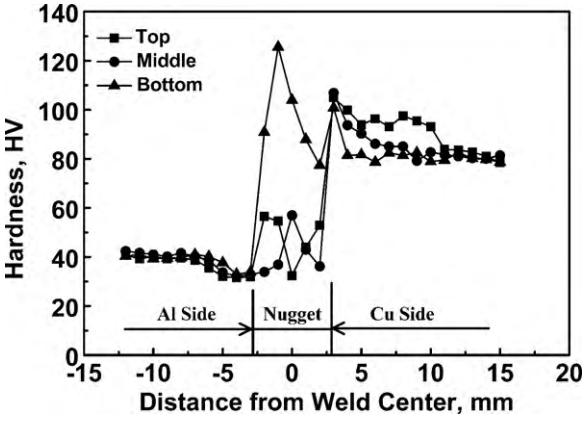

Fig. 5. Hardness profiles along top, middle and bottom lines of transverse cross-section.

Bending properties are especially important for the Al–Cu joints used in electric power industry, and are closely related to the bonding conditions on the Al–Cu interface. Pietras [24] indicated that though good tensile properties were achieved in the FSW Al–Cu joints produced in a wide range of welding parameters, bending properties were not all gratified with the largest bending angle 130°. In our study, the Al–Cu joint could be bent to 180° without fracture (Fig. 6a), showing perfect bending properties. From the magnified SEM image of the interface region (Fig. 6b), no crack was observed in the IMC layer. Moreover, the mini-tension result clearly indicates that the bonding strength of the interface between Al and Cu bulk was higher than 210 MPa, i.e. strength of the PRZ, indicating excellent metallurgical bonding between Al and Cu achieved by FSW.

It is well accepted in the soldering that the presence of the IMCs between the solders and conductor metals is an indication of good metallurgical bonding. A thin, continuous and uniform IMC layer is an essential requirement for good bonding [25]. Moreover,

Table 1
Tensile properties of the FSW Al–Cu joints and the Al base material (BM).

Sample	UTS (MPa)	YS (MPa)	Elongation (%)	Fracture location
Al BM	120	110	18	–
FSW joints				
Large-specimen	110	90	13	HAZ
Mini-specimen	210	140	6	PRZ

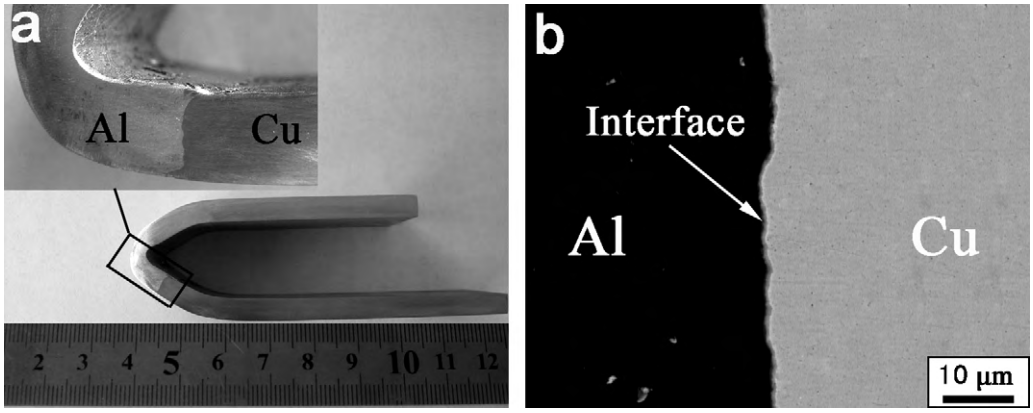

Fig. 6. (a) Macrograph of the joint after bending test, (b) magnified SEM backscattered electron image of the interface region.

Tanaka et al. [26] showed that the bonding strength of the Al–Fe FSW joint was related to the thickness of the IMC layer. So the excellent metallurgical bonding between aluminum and copper generated at the Al–Cu interface was due to the formation of the continuous and uniform Al–Cu IMC layer with a proper thickness of ~1 μm.

Obviously, the nugget zone was significantly strengthened by the fine IMC particles dispersed in the aluminum matrix. For the larger Cu particles in the nugget zone, sound metallurgical bonding with the Al matrix was also achieved through the IMC layers around them. Furthermore, the bonding strength of the Al–Cu interface was greatly enhanced by the formation of the thin, continuous and uniform IMC layer. Therefore, excellent mechanical performance was achieved in the present FSW Al–Cu joint.

4. Conclusions

In summary, the following conclusions are reached:

1. 1060 aluminum alloy and commercial pure copper were successfully friction stir welded by offsetting the tool into the aluminum side. The PRZ formed in the bottom of the nugget zone had a composite structure with variously sized particles dispersed in the Al matrix.
2. The UTS of the composite structure was as high as 210 MPa and the hardness increased substantially due to the strengthening effect of the Al–Cu IMC particles. The reinforcing particles were mainly composed of Al_2Cu, Al_4Cu_9, and few AlCu particles.
3. An excellent metallurgical bonding with a bonding strength being higher than 210 MPa and 180° bending without fracture was generated at the Al–Cu interface. This is due to the formation of a continuous and uniform IMC layer with a proper thickness of ~1 μm, and the IMC layer consisted of Al_2Cu and Al_4Cu_9 sub-layers.

Acknowledgments

This work was supported by (a) the National Outstanding Young Scientist Foundation of China under grant no. 50525103 and (b) the Hundred Talents Program of Chinese Academy of Sciences.

References

[1] Z. Sun, Int. J. Mater. Prod. Technol. 10 (1995) 16–26.
[2] W.B. Lee, Y.M. Yeon, D.U. Kim, S.B. Jung, Mater. Sci. Technol. 19 (2003) 773–778.
[3] Y. Li, P. Liu, J. Wang, H. Ma, Mater. Res. Innovations 11 (2007) 23–26.
[4] M. Nakamura, Y. Yonezawa, T. Nakanishi, K. Kondo, Wire J. 10 (1977) 71–78.
[5] B. Gulenc, Mater. Des. 29 (2008) 275–278.
[6] E.R. Wallach, G.J. Davies, Met. Technol. 4 (1977) 183–190.
[7] V.L.A. da Silveira, A.G. de, O.S. Mury, W.A. Mannheimer, Microstruct. Sci. 14 (1987) 277–287.
[8] C.Y. Chen, H.L. Chen, W.S. Hwang, Mater. Trans. 47 (2006) 1232–1239.
[9] R.S. Mishra, Z.Y. Ma, Mater. Sci. Eng. R. 50 (2005) 1–78.
[10] W.M. Thomas, E.D. Nicholas, J.C. Needham, M.G. Murch, P. Templesmith, C.J. Dawes, G.B. Patent Application No. 9125978.8 (December 1991).
[11] H. Uzun, C.D. Donne, A. Argagnotto, T. Ghidini, C. Gambaro, Mater. Des. 26 (2005) 41–46.
[12] P. Liu, Q.Y. Shi, X.D. Wang, W. Wang, X. Wang, Mater. Lett. 62 (2008) 4106–4108.
[13] J.C. Yan, Z.W. Xu, Z.Y. Li, L. Li, S.Q. Yang, Scripta Mater. 53 (2005) 585–589.
[14] W.B. Lee, S.B. Jung, Mater. Res. Innovations 8 (2004) 93–96.
[15] R. Zettler, Adv. Eng. Mater. 8 (2006) 415–421.
[16] J.H. Ouyang, E. Yarrapareddy, R. Kovacevic, J. Mater. Process. Technol. 172 (2006) 110–122.
[17] Y.S. Stao, S.H.C. Park, M. Michiuchi, H. Kokawa, Scripta Mater. 50 (2004) 1233–1236.
[18] C.J. Hsu, P.W. Kao, N.J. Ho, Scripta Mater. 53 (2005) 341–345.
[19] C.J. Hsu, C.Y. Chang, P.W. Kao, N.J. Ho, C.P. Chang, Acta Mater. 54 (2006) 5241–5249.
[20] I.S. Lee, P.W. Kao, N.J. Ho, Intermetallics 16 (2008) 1104–1108.
[21] ASM Handbooks, vol.3, Alloy Phase Diagrams, ASM International, Materials Park, OH, 2002.
[22] H.G. Jiang, J.Y. Dai, H.Y. Tong, B.Z. Ding, Q.H. Song, Z.Q. Hu, J. Appl. Phys. 74 (1993) 6165–6169.
[23] X.K. Peng, R. Wuhrer, G. Heness, W.Y. Yeung, J. Mater. Sci. 34 (1999) 2029–2038.
[24] A. Pietras, Weld. World 49 (2005) 122–133.
[25] T. Laurila, V. Vuorinen, J.K. Kivilahti, Mater. Sci. Eng. R. 49 (2005) 1–60.
[26] T. Tanaka, T. Morishige, T. Hirata, Scripta Mater. 61 (2009) 756–759.